Electronic Supplementary Material (ESI) for Physical Chemistry Chemical Physics.

Supporting Information

Quest on Singlet Fission of Organic Sulfur-Containing Systems in the Higher Lying Singlet Excited State: An Application Prospect of Anti-Kasha Rule

Chun-Hao Huang[1], *Chi-Chi Wu*[2], *Elise Y. Li*[1]* *and Pi-Tai Chou*[2]*

[1]Department of Chemistry, National Taiwan Normal University, Taipei, 11677, Taiwan

[2]Department of Chemistry, National Taiwan University, Taipei, 10617, Taiwan

‘

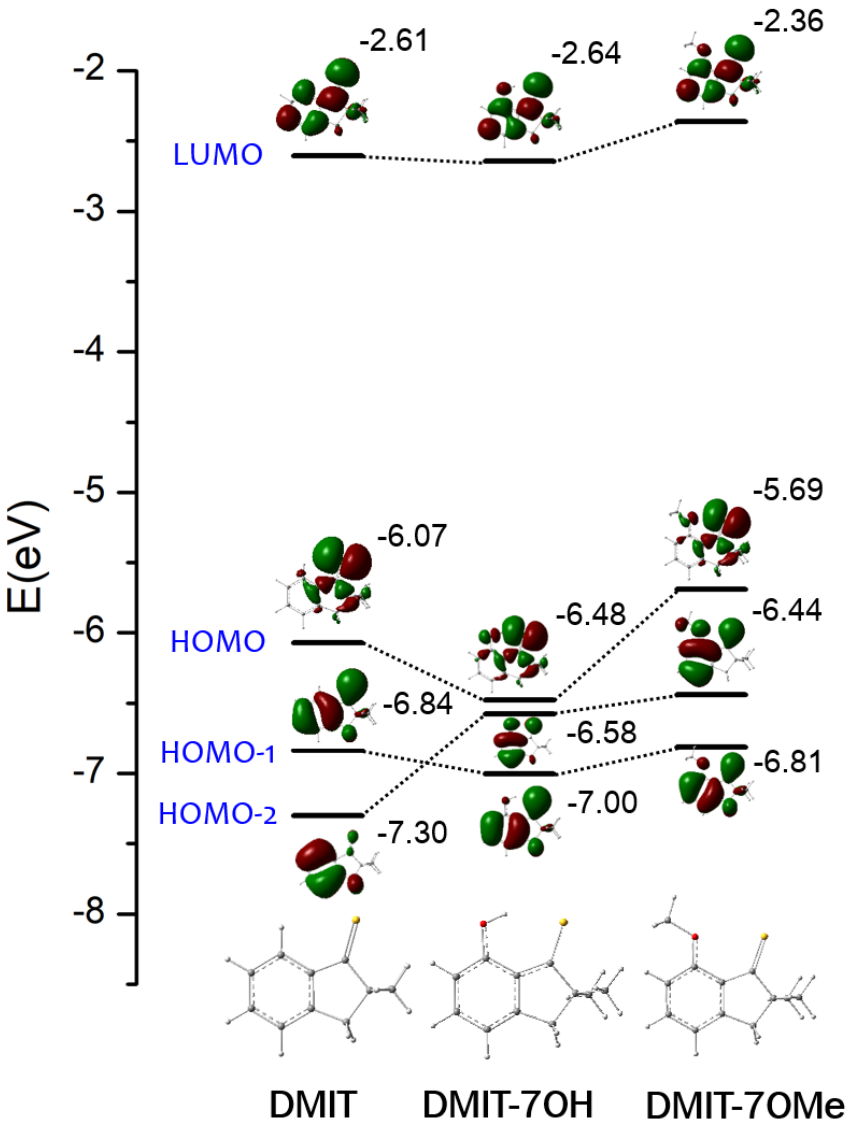

Figure S1. The molecular orbitals and their relative energy alignment at the optimized S_0 geometry of **DMIT**, **DMIT-7OH** and **DMIT-7OMe**.

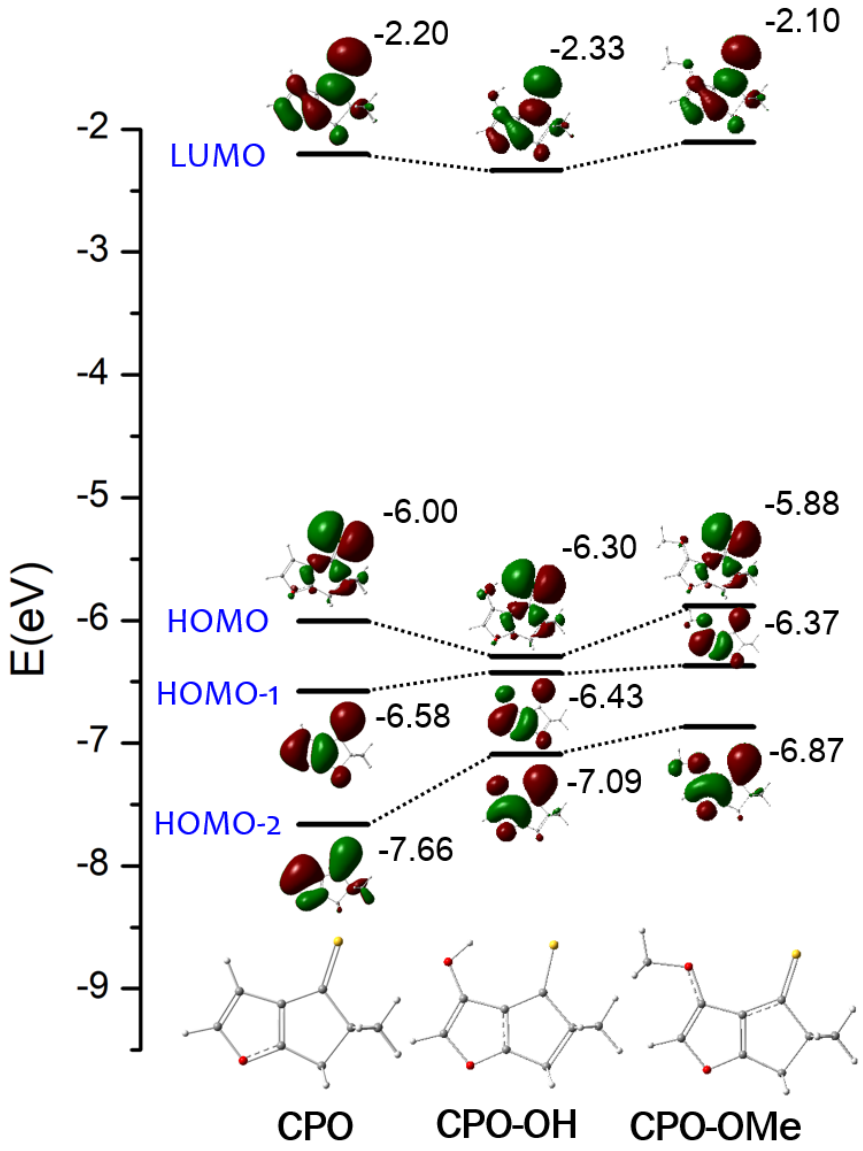

Figure S2. The molecular orbitals and their relative energy alignment at the optimized S_0 geometry of **CPO**, **CPO-OH** and **CPO-OMe**.

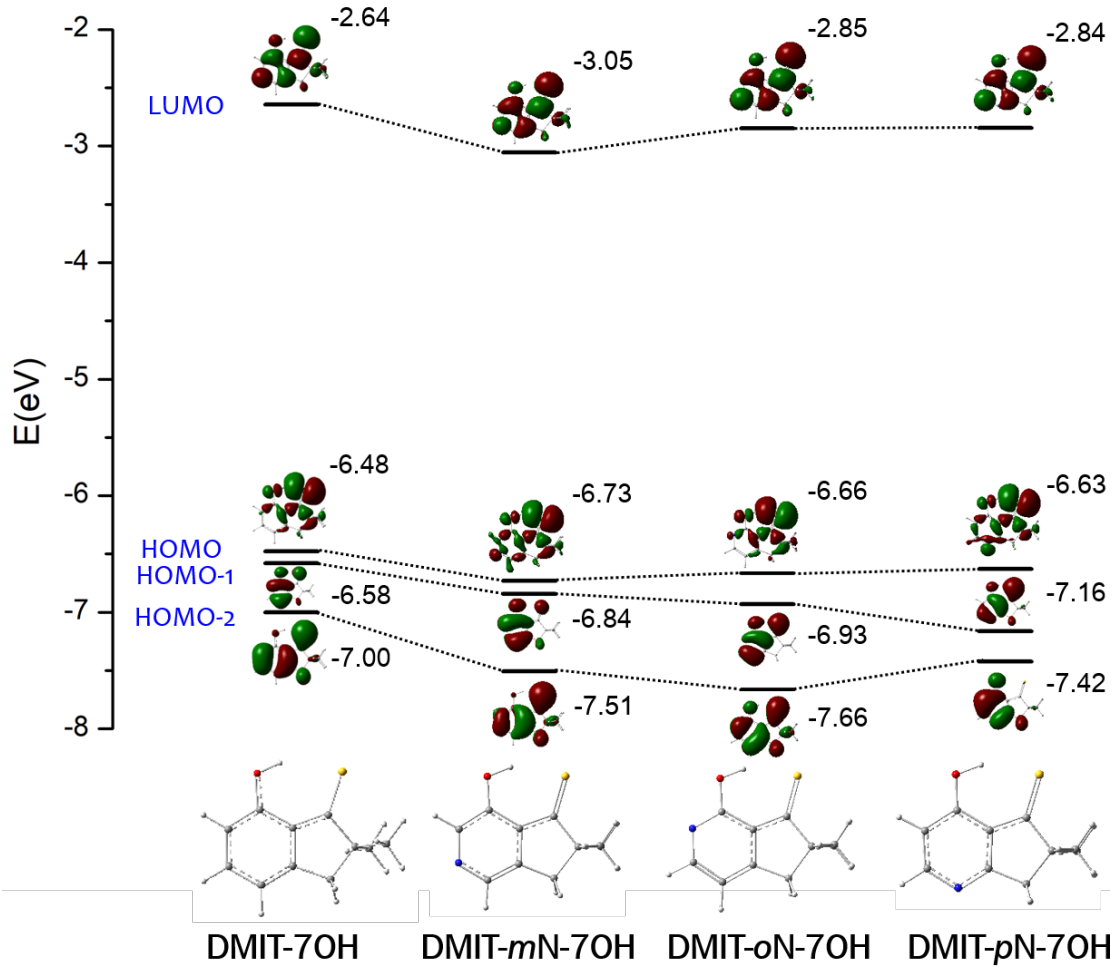

Figure S3. The molecular orbitals and their relative energy alignment at the optimized S_0 geometry of **DMIT-7OH** and its derivatives with nitrogen substituted at *meta*-, *ortho*- or *para*- position.

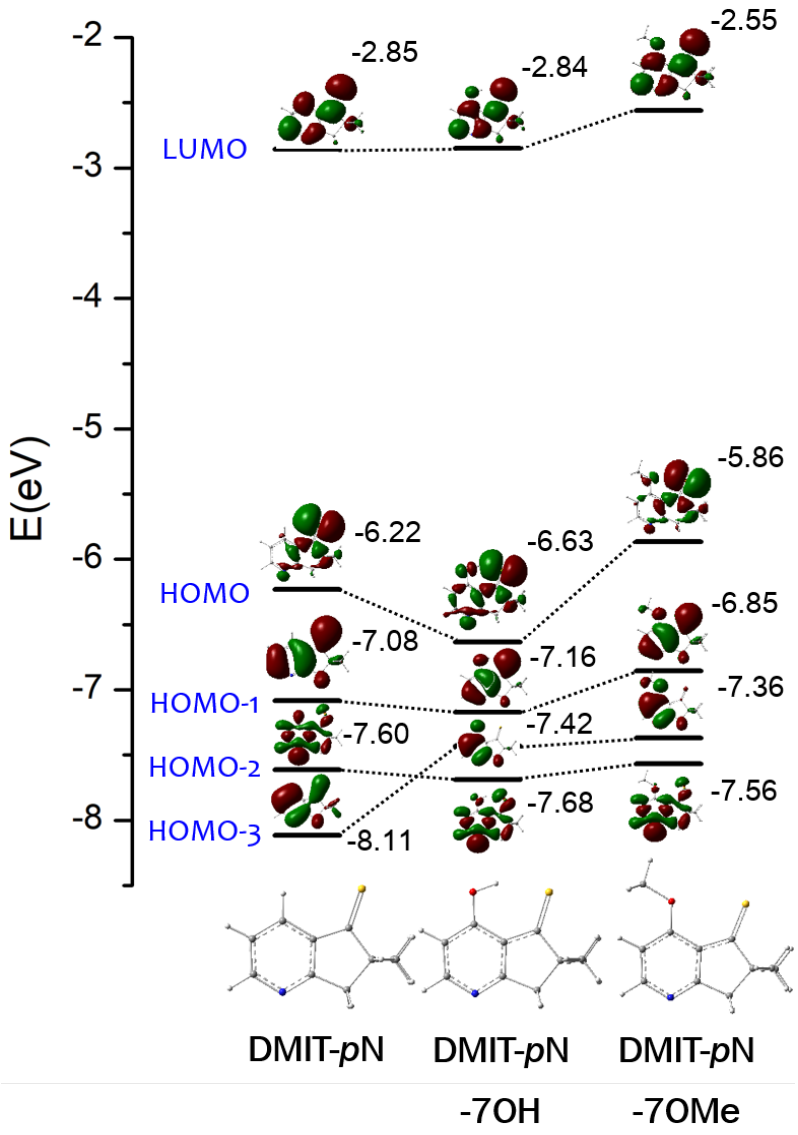

Figure S4. The molecular orbitals and their relative energy alignment at the optimized S_0 geometry of the **DMIT** series.

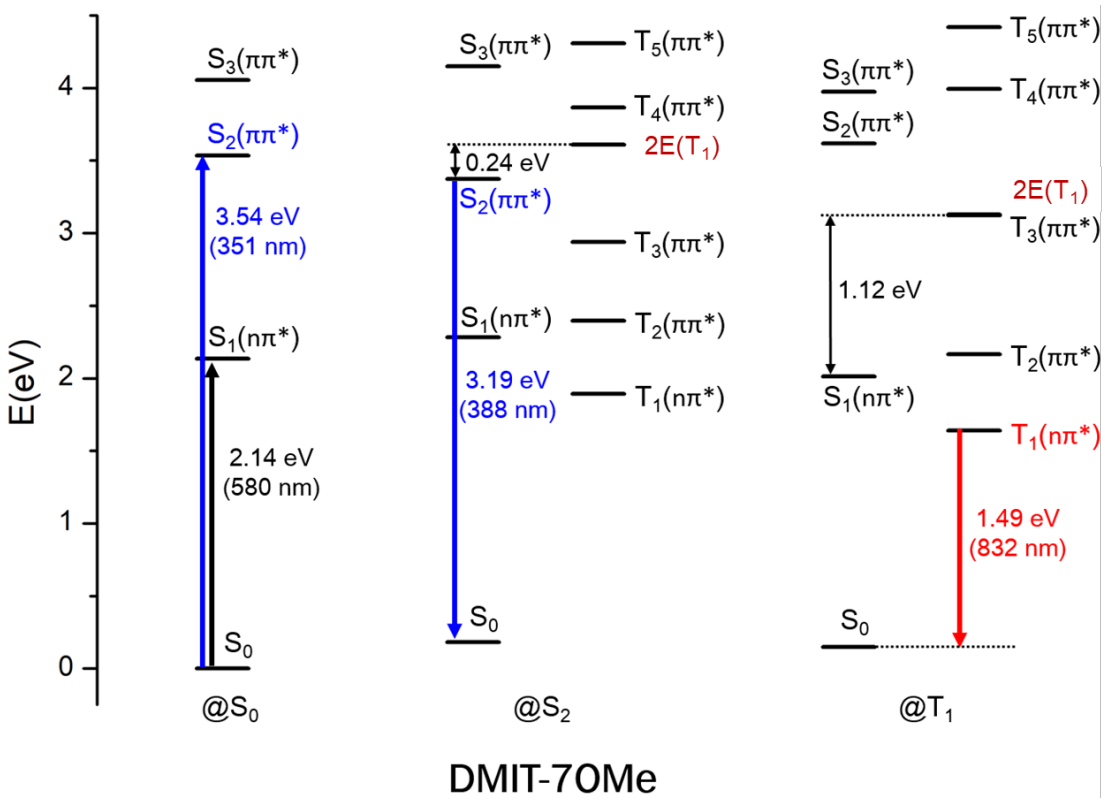

Figure S5. The detailed energy diagram of **DMIT-7OMe** at the optimized S_0, S_2 and T_1 geometries.

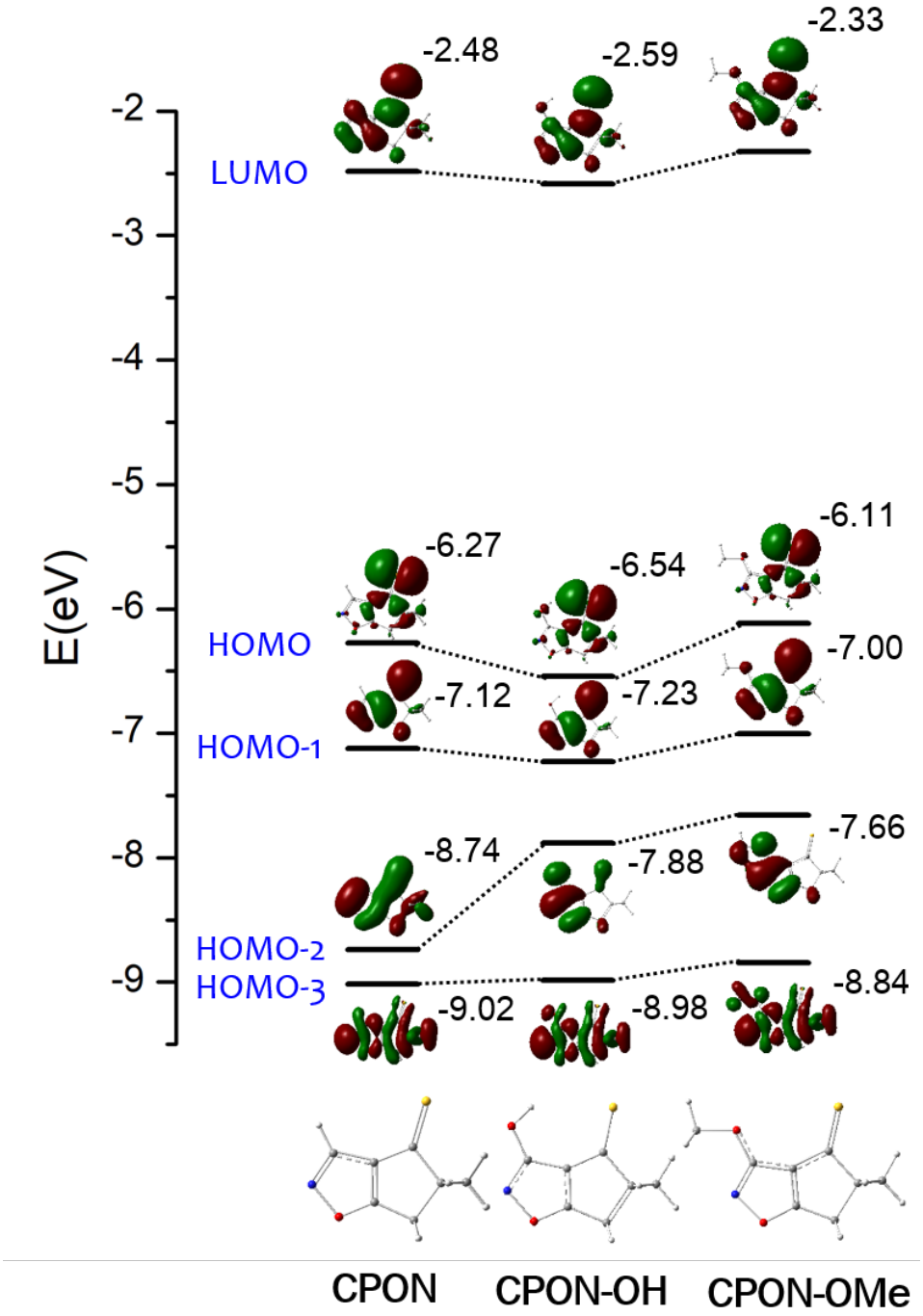

Figure S6. The molecular orbitals and their relative energy alignment at the optimized S_0 geometry of the **CPO** series.

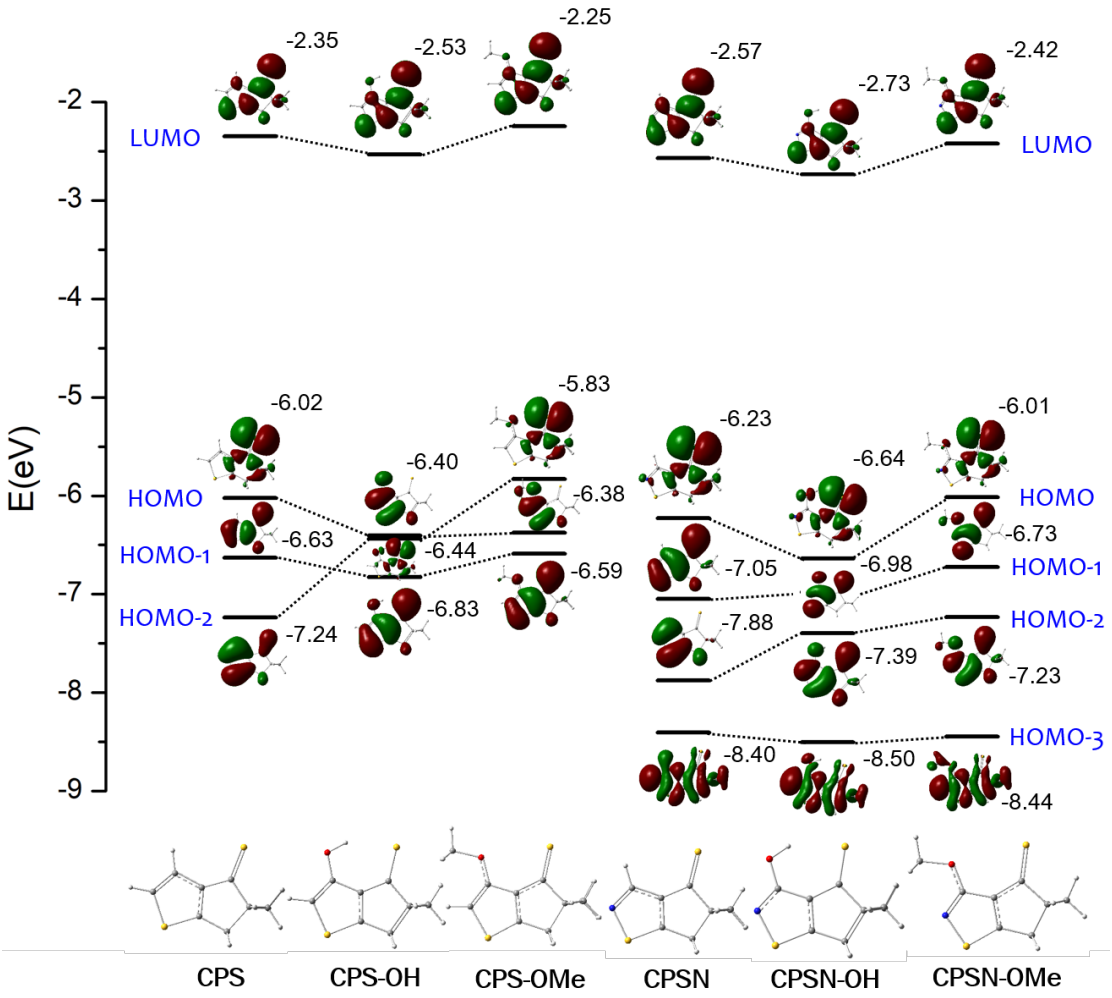

Figure S7. The molecular orbitals and their relative energy alignment at the optimized S_0 geometry of the **CPS** series.

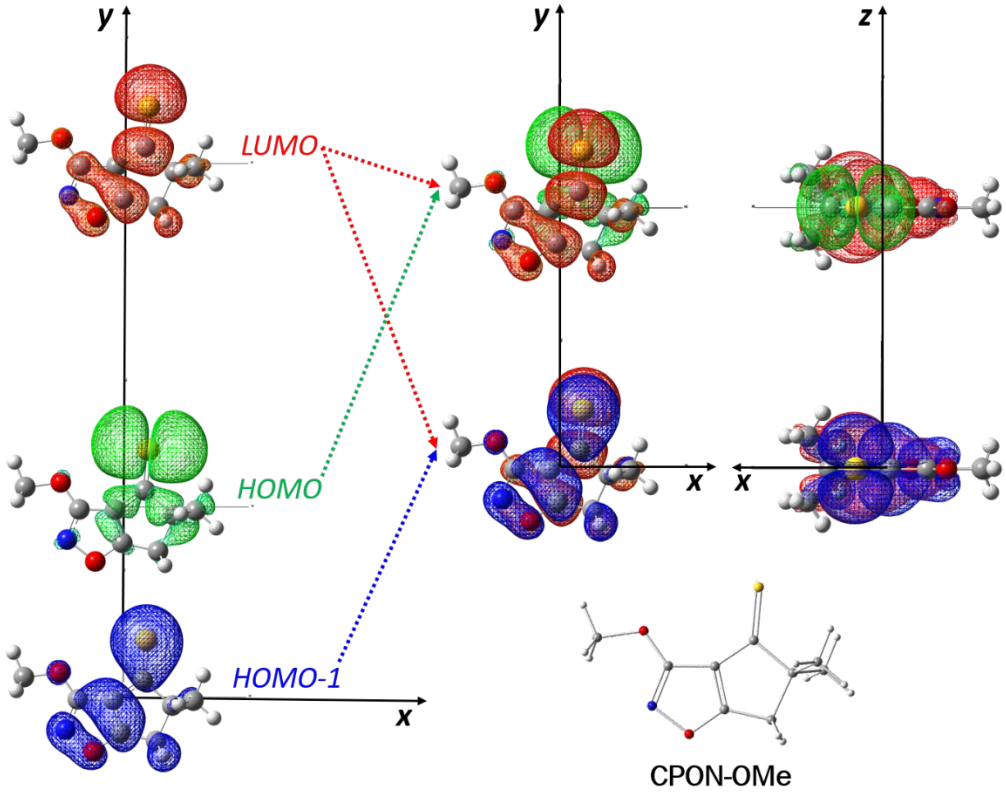

Figure S8. Top view and side view of different frontier molecular orbitals in CPON-OMe mapped together with total density isovalue = 0.02.

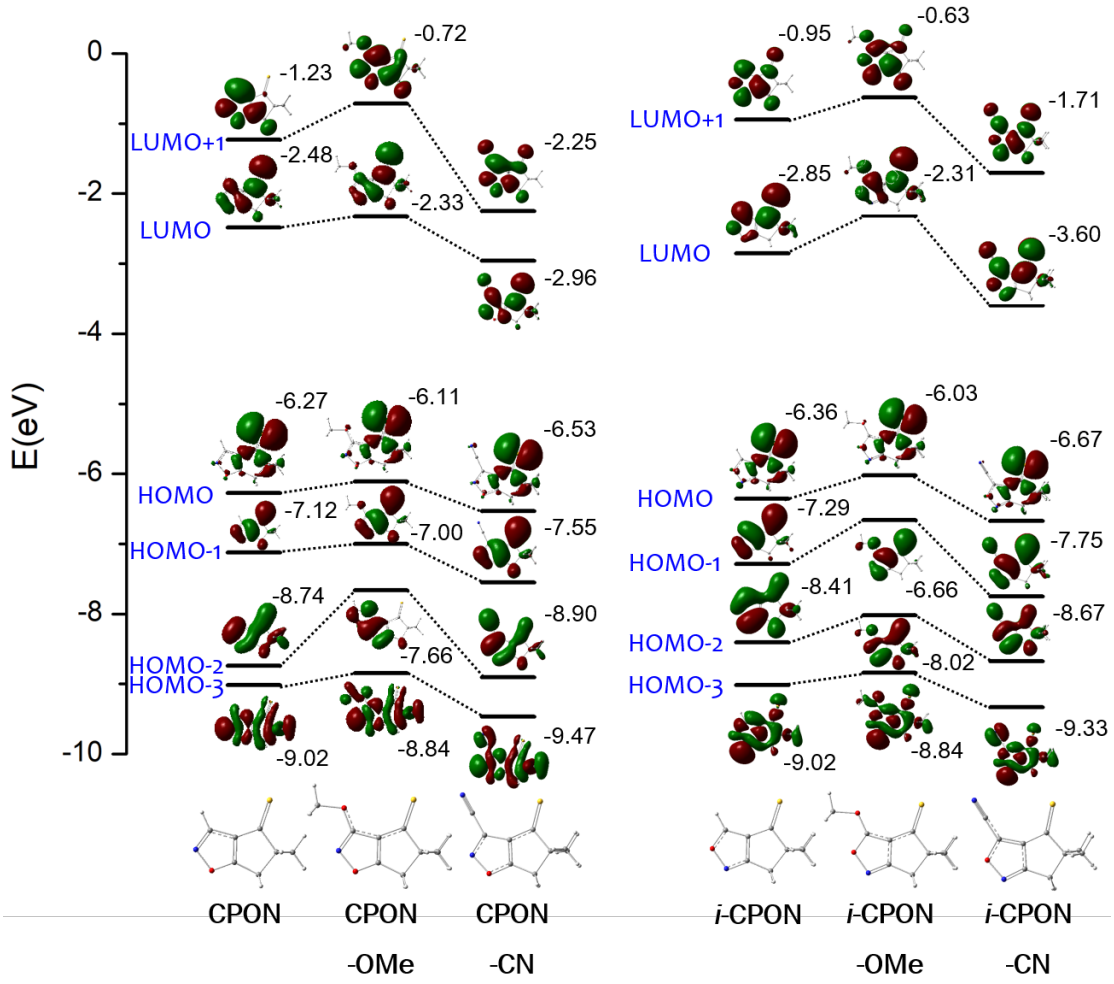

Figure S9. The molecular orbitals and their relative energy alignment at the optimized S_0 geometry of the **CPON** and ***i*-CPON** series.

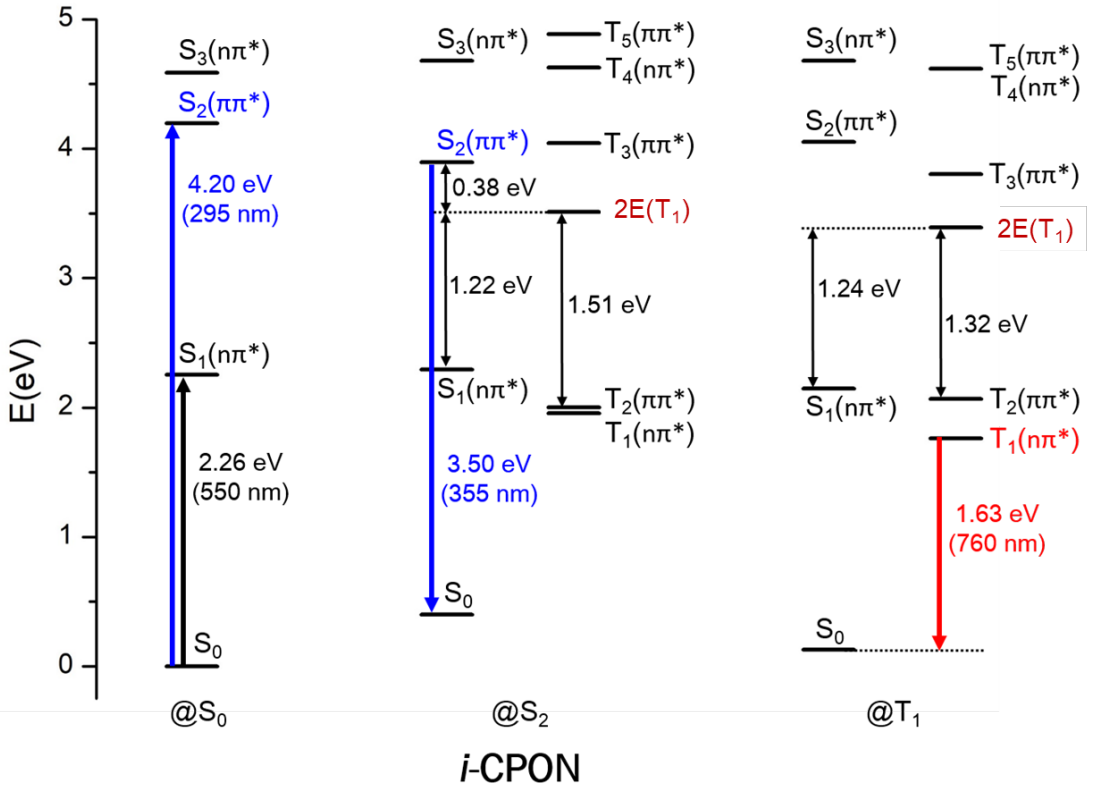

Figure S10. The detailed energy diagram at the optimized S_0, S_2 and T_1 geometries of ***i*-CPON**.

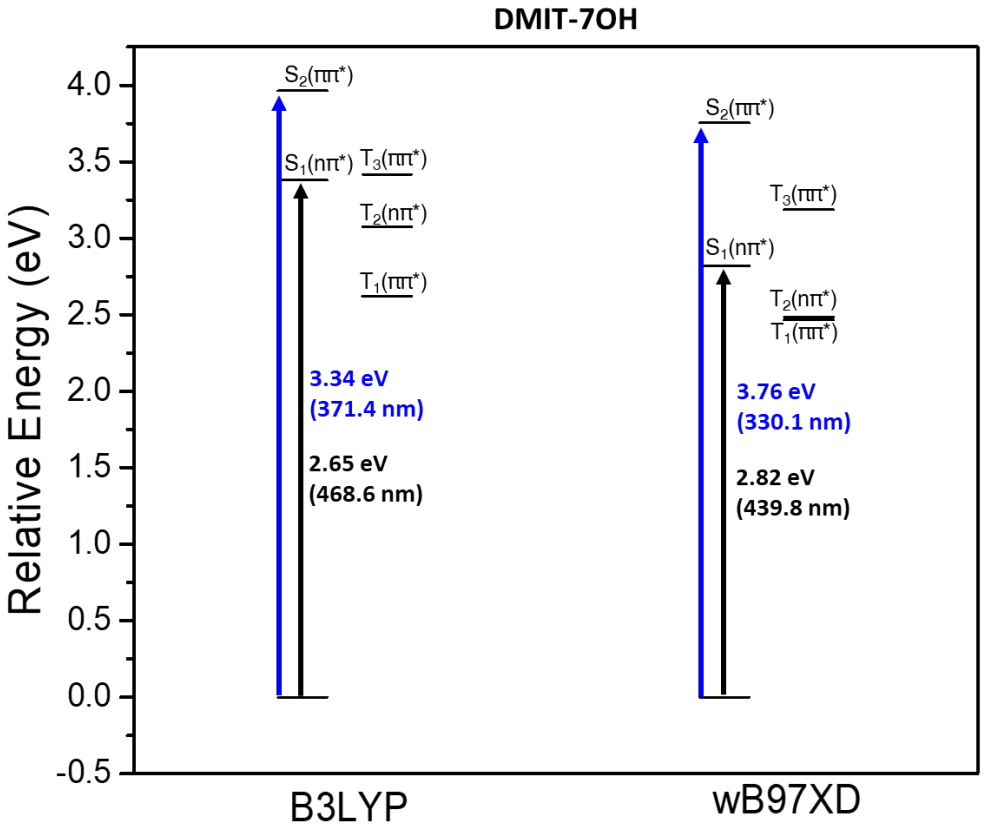

Figure S11. The energy diagram at the optimized S_0 geometries of **DMIT-7OH** with b3lyp and ωB97XD

Table S1. Calculated excitation data at the optimized S_0 geometry of the **DMIT** derivatives.

Compound	Excited state	Energy (eV)	Contribution	Character	$\Delta E(S_2\text{-}S_1)$ E(eV)
DMIT	S_1	2.26	H → L (0.99)	nπ*	1.63
	S_2	3.89	H-1 → L (0.77)	ππ*	
			H-2 → L (0.19)		
	T_1	1.65	H → L (0.99)	nπ*	
	T_2	1.95	H-1 → L (0.94)	ππ*	
DMIT-7OH	S_1	2.65	H → L (0.99)	nπ*	0.7
	S_2	3.34	H-1 → L (0.93)	ππ*	
	T_1	1.95	H → L (0.97)	nπ*	
	T_2	2.18	H-1 → L (0.64)	ππ*	
			H-2 → L (0.31)		
DMIT-7OMe	S_1	2.14	H → L (0.99)	nπ*	1.4
	S_2	3.54	H-1 → L (0.82)	ππ*	
			H-2 → L (0.16)		
	T_1	1.49	H → L (0.99)	nπ*	
	T_2	2.02	H-1 → L (0.86)	ππ*	
			H-2 → L (0.1)		

DMIT-*p*N	S_1	2.19	H → L (0.99)	nπ*	1.54
	S_2	3.73	H-2 → L (0.98)	σπ*	
	S_3	3.90	H-1 → L (0.95)	ππ*	
DMIT–*m*N	S_1	2.48	H → L (0.99)	nπ*	0.73
-7OH	S_2	3.21	H-1 → L (0.97)	ππ*	
	S_3	3.55	H-3 → L (0.97)	σπ*	
DMIT-*o*N	S_1	2.63	H → L (0.99)	nπ*	1
-7OH	S_2	3.63	H-1 → L (0.91)	ππ*	
	S_3	3.9	H-3 → L (0.98)	σπ*	
DMIT-*p*N	S_1	2.60	H → L (0.99)	nπ*	1.23
-7OH	S_2	3.83	H-3 → L (0.98)	σπ*	
	S_3	3.86	H-2 → L (0.75)	ππ*	
			H-1 → L (0.22)		
DMIT-*p*N	S_1	2.12	H → L (0.99)	nπ*	1.85
-7OMe	S_2	3.97	H-1 → L (0.79)	ππ*	
			H-2 → L (0.19)		
	S_3	3.99	H-3 → L (0.97)	σπ*	

Table S2. Calculated excitation data at the optimized S_0 geometry of the **CPO** series.

Compound	Excited state	Energy (eV)	Contribution	Character	$\Delta E(S_2\text{-}S_1)$ E(eV)
CPO	S_1	2.53	H → L (1)	nπ*	1.53
	S_2	4.06	H-1 → L (0.93)	ππ*	
	T_1	1.96	H → L (0.99)	nπ*	
	T_2	2.16	H-1 → L (0.91)	ππ*	
CPO-OH	S_1	2.7	H → L (1)	nπ*	0.77
	S_2	3.47	H-1 → L (0.9)	ππ*	
	T_1	2.04	H → L (0.96)	nπ*	
	T_2	2.15	H-1 → L (0.59)	ππ*	
			H-2 → L (0.34)		
CPO-OMe	S_1	2.5	H → L (1)	nπ*	1.16
	S_2	3.66	H-1 → L (0.84)	ππ*	
			H-2 → L (0.15)		
	T_1	1.92	H → L (0.99)	nπ*	
	T_2	2.17	H-1 → L (0.64)	ππ*	
			H-2 → L (0.36)		

CPON	S_1	2.5	H → L (1)	nπ*	1.79
	S_2	4.29	H → L+1 (1)	nπ*	
	S_3	4.36	H-1 → L (0.96)	ππ*	
	S_6	5.57	H-3 → L (0.99)	σπ*	
CPON	S_1	2.68	H → L (1)	nπ*	1.67
-OH	S_2	4.35	H-1 → L (0.88)	ππ*	
	S_6	5.45	H-3 → L (0.99)	σπ*	
CPON	S_1	2.50	H → L (1)	nπ*	1.93
-OMe	S_2	4.42	H-1 → L (0.96)	ππ*	
	S_7	5.58	H-3 → L (0.99)	σπ*	

Table S3. Calculated excitation data at the optimized S_0 geometry of the **CPS** series.

Compound	Excited state	Energy (eV)	Contribution	Character	$\Delta E(S_2\text{-}S_1)$ E(eV)
CPS	S_1	2.43	H → L (0.99)	nπ*	1.54
	S_2	3.97	H-1 → L (0.83)	ππ*	
			H-2 → L (0.14)		
CPS-OH	S_1	2.69	H-1 → L (0.99)	nπ*	0.48
	S_2	3.16	H → L (0.98)	ππ*	
CPS-OMe	S_1	2.35	H → L (0.99)	nπ*	1.07
	S_2	3.42	H-1 → L (0.98)	ππ*	

CPSN	S_1	2.4	H → L (0.99)	nπ*	1.61
	S_2	4	H → L+1 (0.99)	nπ*	
	S_3	4.18	H-1 → L (0.95)	ππ*	
	S_5	4.9	H-3 → L (0.99)	σπ*	
CPSN-OH	S_1	2.68	H → L (0.99)	nπ*	1.01
	S_2	3.69	H-1 → L (0.82)	ππ*	
			H-2 → L (0.17)		
	S_5	4.82	H-3 → L (0.97)	σπ*	
CPSN-OMe	S_1	2.35	H → L (0.99)	nπ*	**1.46**
	S_2	3.81	H-1 → L (0.82)	ππ*	
			H-2 → L (0.17)		
	S_7	5.07	H-3 → L (0.86)	σπ*	

Table S4. Calculated excitation data at the optimized S_0 geometry of the **CPON** and ***i*-CPON** series.

Compound	Excited state	Energy (eV)	Contribution	Character	$\Delta E(S_2\text{-}S_1)$ E(eV)
CPON	S_1	2.5	H → L (1)	nπ*	1.79
	S_2	4.29	H → L+1 (1)	nπ*	
	S_3	4.36	H-1 → L (0.96)	ππ*	
CPON-OMe	S_1	2.5	H → L (1)	nπ*	1.93
	S_2	4.42	H-1 → L (0.96)	ππ*	
	S_3	4.57	H-2 → L (0.99)	ππ*	
CPON-CN	S_1	2.34	H → L (0.96)	nπ*	1.17
	S_2	3.51	H → L+1 (0.97)	nπ*	
	S_3	4.22	H-1 → L (0.9)	ππ*	

***i*-CPON**	S_1	2.26	H → L (0.99)	nπ*	1.94
	S_2	4.2	H-1 → L (0.98)	ππ*	
	S_3	4.59	H → L+1 (0.98)	nπ*	
***i*-CPON**	S_1	2.45	H → L (0.99)	nπ*	1.59
-OMe	S_2	4.04	H-1 → L (0.97)	ππ*	
	S_3	4.64	H → L+1 (0.99)	nπ*	
***i*-CPON**	S_1	1.93	H → L (0.98)	nπ*	1.99
-CN	S_2	3.92	H-1 → L (0.99)	ππ*	
	S_3	4.02	H → L+1 (0.97)	nπ*	

Table S5. Theoretical data of the designed systems in this study at the optimized S_0, S_2 and T_1 geometries and the experimental excitation data of the cofacial perylene dimer.

[a] calculated from $E(S_2)@S_0$ (eV) - $2E(T_1)@T_1$ (eV)

Compound	**DMIT-*p*N -7OMe**	**CPON -OMe**	***i*-CPON**	cofacial perylene dimer [1]
$E(S_2)@S_0$ (eV)	3.97	4.42	4.2	4.96
$E(T_1)@T_1$ (eV)	1.49	1.91	1.63	1.51
Heat loss[a]	0.99	0.6	0.94	**1.94**

Table S6. Spin-orbit couplings calculated as root mean squares (cm^{-1}) at S_2-optimized structure of DMIT-derivatives

<S|Hso|T>	T_3 (ΔE_{ST})[a]	T_4 (ΔE_{ST})	T_5 (ΔE_{ST})	T_6(ΔE_{ST})
DMIT	0.67 (0.21)	0.92 (-0.22)	0.62 (-0.96)	13.34 (-1.00)
DMIT-7OMe	2.28 (0.43)	1.42 (-0.49)	2.84 (-0.93)	11.10 (-1.35)
DMIT-pN	1.91 (0.14)	18.21 (-0.88)	1.16 (-1.24)	10.44 (-1.28)
DMIT-pN-7OMe	1.51 (1.79)	9.34 (1.27)	12.02 (0.67)	1.08 (0.41)
CPO	23.32(-0.23)	13.30(-1.01)	24.24(-1.69)	4.59(-2.41)
CPO-OMe	2.11 (0.30)	2.08 (-0.45)	13.3 (0.94)	7.76 (-1.35)
CPON-OMe	0.54 (0.30)	0.30 (-0.32)	8.50 (-1.64)	17.70 (-1.68)
i-CPON	0.26 (-0.26)	117.62 (-0.83)	0.12 (-1.06)	87.61 (-1.23)

[a] $\Delta E_{ST}=(E_{S2}-E_{Tn})$ at S_2-optimized structure

Table S7. Calculated excitation data with ωB97XD at the optimized geometries of the DMIT-7OH series.

Structure	Excited state	Energy (eV)	Contribution	Character	$\Delta E(S_2\text{-}S_1)$ E(eV)
	S_1	2.82	H-1 → L (0.94)	nπ*	
	S_2	3.76	H → L (0.96)	ππ*	
	T_1	2.47	H-2 → L (0.39)	ππ*	
@S_0-opt			H-1 → L (0.09)	nπ*	0.94
			H → L (0.46)	ππ*	
	T_2	2.48	H-2 → L (0.07)	ππ*	
			H-1 → L (0.85)	nπ*	
	S_1	2.58	H → L (0.95)	nπ*	
	S_2	3.75	H-1 → L (0.95)	ππ*	
	T_1	2.22	H-2 → L (0.08)	ππ*	
			H-1 → L (0.17)	ππ*	
@S_1-opt			H → L (0.69)	nπ*	1.17
	T_2	2.28	H-2 → L (0.30)	ππ*	
			H-1 → L (0.39)	ππ*	
			H → L (0.25)	nπ*	
	S_1	2.85	H-1 → L (0.96)	nπ*	
	S_2	3.38	H → L (0.98)	ππ*	
@S_2-opt	T_1	2.3	H-2 → L (0.40)	ππ*	0.53
			H → L (0.56)	ππ*	
	T_2	2.54	H-1 → L (0.95)	nπ*	

References

(1) W. Ni, G. G. Gurzadyan, J. Zhao, Y. Che, X. Li, and L. Sun, *J. Phys. Chem. Lett.* **2019**, *10*, 2428-2433.